

ON THE VOLUME OF SETS BOUNDED BY REFINABLE FUNCTIONS

JAN HAKENBERG AND ULRICH REIF

ABSTRACT. We present a method for the precise determination of the volume of subsets of \mathbb{R}^d which are bounded by a hypersurface parametrized by a set of refinable functions. The derivation is based on the linear refinement equations rather than on closed form expressions of these functions, which may not be available. In particular, our approach makes it possible to compute the area of planar domains bounded by subdivision curves or the volume of spatial domains bounded by subdivision surfaces.

1. INTRODUCTION

The volume of some subset $\Omega \subset \mathbb{R}^d$ can be determined easily with the help of the divergence theorem if a closed form expression for the parametrization of its boundary is available. However, if the boundary is created by a subdivision scheme, the problem is more delicate. If, for instance, a boundary curve is generated by the four-point scheme, then it is impossible to find a parametrization which is suitable for direct integration. Equally, if a boundary surface is generated by a subdivision algorithm like Catmull-Clark or Loop, then a piecewise analytic representation is known, but there are infinitely many of these pieces. In applications, it may be sufficient to compute a numerical approximation, but convergence rates of standard quadrature schemes are typically low due to the limited regularity of subdivision functions.

In this paper, we present an alternative approach to the problem. It is based on the refinement rules of the representation of the boundary rather than on explicit knowledge of its function values. In fact, our method applies whenever the parametrization of the boundary consists of a finite number of patches each of which is a linear combination of a set of refinable functions. Here, refinability means that there exists a partition of the domain of the patch into subdomains such that the restrictions of the functions to these subdomains can be reparametrized in terms of the functions themselves. This assumption is satisfied for boundaries generated by subdivision schemes, wavelets, or B-splines, but also for more general classes of functions.

The basic idea is the following: Application of the divergence theorem shows that the contribution of a single patch to the total volume of the given set Ω can be expressed by means of a certain multi-linear form M , which has to be determined. After partitioning the domain of the patch, the same contribution is now obtained as the sum over the shares of the subpatches, which in turn can be described in terms of M . In this way, we obtain a linear interrelation between the coefficients of the multi-linear form which, typically, determines M up to scaling. Eventually, the remaining degree of freedom can be calibrated by considering a single special configuration. In Figure 1, we see two cases which can be handled by our framework. On the left hand side, we see a tripod generated from an assembly of four unit cubes by the Catmull-Clark algorithm. The enclosed volume $V \approx 2.504005476$ is given exactly as the quotient of two fairly big integers¹. The subdivision surface on the right is generated from a regular octahedron with all edges length 1 by the algorithm suggested in [10], where the edges of two opposite triangles are tagged to form sharp creases. Here, the enclosed volume is $V = 9\sqrt{2}/56 \approx 0.227284323$.

Date: November 19, 2014.

¹ V equals 401800824426700512529009021773935165102112089658921708365692266292142127089978566394595507008291025740312016930566345611408996475551350555006566604831407569607788986492449554641219821870336717316476247679551629672346929205592993625071348599372485886982248931397015773189041536841679354460766183340033768028257472084982766119564689607412283694545858835385150366631268809254233132555169056767142562957502393768749712436004182071021 divided by 16046323710242313089909175392307959118108021410074742425376177351348347992382685285901785697765860338901271935282090099437828184717866085833813124018343088953677884563654098038825035627833352494074499327159439890167562372988838107467187740355820288057315668957360892263650741951870598031110070042290053682482516290078543763389134227824008775572142274115412160255773388520595334004563330096707755296887477615110463588476731392000.

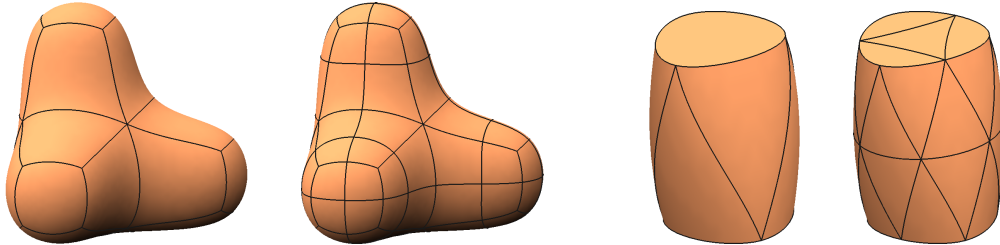


FIGURE 1. Catmull-Clark surface (*left*) and subdivision surface with sharp creases (*right*). The determination of the enclosed volumes is based on the equivalence of a given and the refined representation of the boundary.

The idea which is detailed and generalized in this report appears first in the monograph [19]. Here, Warren and Weimer introduce the basic principle for univariate subdivision schemes and determine the area form corresponding to the four-point scheme without tension. The problem of computing volumes of spatial subsets bounded by subdivision surfaces, which has some relevance in applications, has also been considered before, but using a different approach. In [16], approximate volume formulas for boundaries generated by subdivision schemes are suggested. They are obtained by summing up the volume contributions of a *finite number* of spline rings, and neglecting an infinite number of ever smaller pieces near the extraordinary vertex. The contribution of a single spline ring is assumed to be computable via integration so that, essentially, the approach of Peters and Nasri is restricted to algorithms generalizing B-spline or box spline subdivision. Accurate results for boundaries generated by the Doo-Sabin algorithm are derived by Schwald in [18]. Here, the volume contributions of *all* spline rings are taken into account. This is achieved by eigen-decomposition of the subdivision matrix and the summation of the contributions of certain infinite sequences of scaled eigen-rings, amounting to the summation of geometric series. The volume of the set bounded by the limit surface corresponding to the unit cube is found to be $6241/9920$, showing that the according value $0.629137\dots$ given in [16] is accurate up to the fifth digit.

The paper is organized as follows: In the next section, we develop the fundamental ideas. In particular, we introduce systems of refinable functions, and also systems of *partially* refinable functions, which are useful when analyzing subdivision surfaces in a vicinity of an extraordinary vertex. Further, we discuss how to reduce the possibly high complexity of a given problem by exploiting symmetries. Section 3 is devoted to a discussion of some algorithmic issues. First, we describe the basic strategy. In particular, it is shown how to set up the linear system for the determination of the coefficients of the sought multi-linear form, and how to calibrate the remaining free parameters. Then, we discuss some variants, including the case of partial refinability and the involvement of symmetries. In Section 4, we consider a few special scenarios in order to illustrate the potential of our method in applications. We discuss uniform and non-uniform univariate subdivision schemes, uniform tensor product- and triangle-based schemes, and finally some non-uniform bivariate schemes.

2. FOUNDATION

In this section, we prepare the ground for the computation of volumes by means of alternating multilinear forms and for their explicit determination. After introducing some notation, we elaborate on volumes bounded by hypersurface segments which are parametrized by functions allowing for complete or partial refinement. Also the aspect of symmetry is discussed.

2.1. Notation. Let $\Omega \subset \mathbb{R}^d$ with $d \geq 2$ be a bounded open subset with boundary $\partial\Omega$, the latter being the closure of the finite, disjoint union of *segments*² $\partial\Omega_j$, $j \in J$. Each segment is parametrized over some open, Jordan measurable³ domain $\omega_j \subset \mathbb{R}^{d-1}$ by some function

²Segments of bivariate spline or subdivision surfaces are also called *patches*.

³The Lebesgue measure of the boundary of a Jordan measurable set is 0. Hence, integrals over the set and its closure coincide.

$\mathbf{x}_j : \omega_j \rightarrow \mathbb{R}^d$ in the Sobolev class $H^{1,\infty}$ of functions whose weak first derivative is essentially bounded⁴. That is,

$$\partial\Omega = \bigcup_{j \in J} \overline{\partial\Omega_j}, \quad \partial\Omega_j = \mathbf{x}_j(\omega_j), \quad \partial\Omega_i \cap \partial\Omega_j = \emptyset, \quad i \neq j \in J.$$

The *area element* of $\partial\Omega_j$ is given by

$$dA_j = \|\mathbf{n}_j\| d\lambda, \quad \mathbf{n}_j := \begin{cases} \begin{bmatrix} 0 & 1 \\ -1 & 0 \end{bmatrix} \partial_1 \mathbf{x}_j & \text{if } d = 2 \\ \partial_1 \mathbf{x}_j \wedge \cdots \wedge \partial_{d-1} \mathbf{x}_j & \text{if } d > 2, \end{cases}$$

where λ is the Lebesgue measure on ω_j . The unit normal on that segment is $\mathbf{n}_j^0 := \varepsilon_j \mathbf{n}_j / \|\mathbf{n}_j\|$, where the sign $\varepsilon_j \in \{-1, 1\}$ is chosen such that \mathbf{n}_j^0 is pointing to the exterior of Ω . Now, the divergence theorem yields the formula

$$\text{vol}(\Omega) = \int_{\Omega} 1 d\lambda = \frac{1}{d} \sum_{j \in J} \int_{\partial\Omega_j} \mathbf{x}_j \cdot \mathbf{n}_j^0 dA_j = \frac{1}{d} \sum_{j \in J} \varepsilon_j \int_{\omega_j} \mathbf{x}_j \cdot \mathbf{n}_j d\lambda$$

for the *volume* of Ω . Thus, suppressing subscripts, the problem of determining $\text{vol}(\Omega)$ is reduced to the computation of expressions of the form

$$V(\mathbf{x}) := \frac{1}{d} \int_{\omega} \mathbf{x} \cdot \mathbf{n} d\lambda = \frac{1}{d} \int_{\omega} \det[\mathbf{x}, D\mathbf{x}] d\lambda, \quad \mathbf{x} \in H^{1,\infty}(\omega, \mathbb{R}^d),$$

where $D\mathbf{x} := [\partial_1 \mathbf{x}, \dots, \partial_{d-1} \mathbf{x}]$ is the Jacobian of the map \mathbf{x} . If the components of \mathbf{x} lie in a common, finite dimensional function space, spanned⁵ by functions $b_j : \omega \rightarrow \mathbb{R}$ forming the row vector $B := [b_1, \dots, b_n]$, we write

$$\mathbf{x} = B\mathbf{P} := \sum_{j=1}^n b_j \mathbf{p}^j$$

for certain coefficients $\mathbf{p}^j \in \mathbb{R}^d$, which are regarded as row vectors and stacked to form the matrix $\mathbf{P} \in \mathbb{R}^{n \times d}$. The elements of \mathbf{P} are denoted by p_k^j and its columns by P_k , i.e.,

$$\mathbf{P} = \begin{bmatrix} \mathbf{p}^1 \\ \vdots \\ \mathbf{p}^n \end{bmatrix} = (p_k^j)_{j,k} = [P_1, \dots, P_d].$$

Using standard multi-index notation, we write

$$\mathbf{p}^\alpha := p_1^{\alpha_1} \cdots p_d^{\alpha_d}, \quad \alpha = [\alpha_1, \dots, \alpha_d] \in \Gamma := \{1, \dots, n\}^d.$$

2.2. Volumes as Multilinear Forms. Going back to the definition of V , we find

$$V(B\mathbf{P}) = \sum_{\alpha \in \Gamma} \det[P_{\alpha_1}, \dots, P_{\alpha_d}] \tilde{m}_\alpha, \quad \tilde{m}_\alpha := \frac{1}{d} \int_{\omega} b_{\alpha_1} \partial_1 b_{\alpha_2} \cdots \partial_{d-1} b_{\alpha_d} d\lambda.$$

We expand the determinants and collect products containing \mathbf{p}^α to obtain the representation of $V(B\mathbf{P})$ in terms of some *d-linear form* M in \mathbb{R}^n ,

$$(1) \quad V(B\mathbf{P}) = M \cdot \mathbf{P} := \sum_{\alpha \in \Gamma} m_\alpha \mathbf{p}^\alpha, \quad m_\alpha := \sum_{\pi \in \Pi_d} \det(\pi) \tilde{m}_{\alpha\pi}.$$

Here, Π_d denotes the set of all $d \times d$ permutation matrices, i.e., the vector-matrix product $\alpha\pi$ is a rearrangement of the entries of α . For instance, in the curve case $d = 2$, it is

$$(2) \quad m_\alpha = \frac{1}{2} \int_{\omega} (b_{\alpha_1} b'_{\alpha_2} - b_{\alpha_2} b'_{\alpha_1}) d\lambda.$$

When permuting the coordinates of \mathbf{P} , the resulting value of V coincides with the given one up to sign,

$$V(B\mathbf{P}\pi) = \det(\pi) V(B\mathbf{P}), \quad \pi \in \Pi_d.$$

⁴This implies that the functions \mathbf{x}_j are continuous and that all integrals appearing in the following are well defined. The slightly weaker condition $\mathbf{x}_j \in H^{1,d-1}$ would be equally sufficient for that purpose.

⁵Typically, the functions b_1, \dots, b_n are linearly independent and thus form a basis, but this fact is not needed here.

Hence, as could also be seen directly from the definition, the d -linear form M is *alternating*, i.e., $M \cdot (\mathbf{P}\pi) = \det(\pi)M \cdot \mathbf{P}$. The space of all such forms is denoted by

$$\mathcal{S} := \{M = (m_\alpha)_{\alpha \in \Gamma} : m_\alpha = \det(\pi)m_{\alpha\pi}, \pi \in \Pi_d\},$$

and can be parametrized as follows: Let $\Lambda := \{\lambda \in \Gamma : \lambda_1 < \lambda_2 < \dots < \lambda_d\}$ be the set of strictly monotone increasing multi-indices. The number of elements in Λ is $|\Lambda| = \binom{n}{d}$. With $\delta_{\alpha,\beta}$ the Kronecker symbol, let $E_\alpha := (\delta_{\alpha,\beta})_{\beta \in \Gamma}$ be the *unit form* with all coefficients being 0, except for that with index $\alpha \in \Gamma$. For $\lambda \in \Lambda$, the alternating d -linear form S_λ is defined by composing the unit forms corresponding to the permutations of λ . More precisely,

$$S_\lambda := \sum_{\pi \in \Pi_d} \det(\pi)E_{\lambda\pi} \in \mathcal{S}.$$

Since $\text{span}\{S_\lambda : \lambda \in \Lambda\} = \mathcal{S}$, there exist coefficients $c_\lambda \in \mathbb{R}$ such that the sought d -linear form is $M = \sum_{\lambda \in \Lambda} c_\lambda S_\lambda$.

2.3. Refinability. Of course, if the functions $B = [b_1, \dots, b_n]$ are known explicitly, the coefficients m_α can be determined by integration. However, this must not be taken for granted: If, for instance, the functions are generated by a recursive procedure like subdivision, direct access to the values of B might be difficult or even impossible. But even in this case, the problem can be solved if the functions B allows refinement in the following sense:

Definition 1. *The system B is called refinable over ω if there exists a finite family of pairs (T_k, A_k) , $k \in K$, consisting of diffeomorphisms $T_k : \omega \rightarrow \tau_k \subset \omega$ with $\det DT_k > 0$ and constant $(n \times n)$ -matrices A_k with the following properties:*

- *Up to closure, the images τ_k form a partition of ω ,*

$$\bar{\omega} = \bigcup_{k \in K} \bar{\tau}_k, \quad \tau_k \cap \tau_\ell = \emptyset, \quad k \neq \ell \in K.$$

- *B restricted to τ_k can be reparametrized over ω by means of itself,*

$$B \circ T_k = BA_k^t, \quad k \in K.$$

Typically, the maps T_k are similarities, and all images $\tau_k, k \in K$, are congruent. With m the cardinality of K , this case is referred to as an *m-split*. However, the following example shows that also more general types of partitions are feasible.

Example 1. The functions $B(t) = [1, t, t^2]$ are refinable over $\omega = (0, 1)$ with

$$T_1(t) = t/3, \quad T_2(t) = (2t + 1)/3, \quad A_1 = \begin{bmatrix} 1 & 0 & 0 \\ 0 & 1/3 & 0 \\ 0 & 0 & 1/9 \end{bmatrix}, \quad A_2 = \begin{bmatrix} 1 & 0 & 0 \\ 1/3 & 2/3 & 0 \\ 1/9 & 4/9 & 4/9 \end{bmatrix}.$$

The partition of ω into $\tau_1 = (0, 1/3), \tau_2 = (1/3, 1)$ is asymmetric, but of course, this choice is not unique. In particular, the usual two-split $T_1(t) = t/2, T_2(t) = (1 + t)/2$ is equally possible. \square

Now, the following result is as elementary as crucial:

Theorem 2. *Let the functions B be refinable according to the preceding definition. Then*

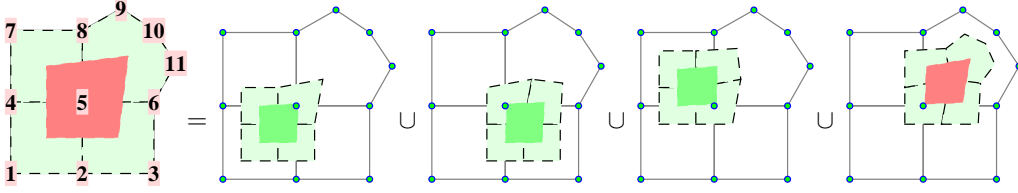
$$(3) \quad M = \sum_{k \in K} M[A_k],$$

where the d -linear form $M[A]$ is defined by

$$M[A] \cdot \mathbf{P} := M \cdot (A^t \mathbf{P}), \quad \mathbf{P} \in \mathbb{R}^{n \times d}.$$

Its coefficient with index $\alpha \in \Gamma$ is given by

$$(4) \quad (M[A])_\alpha = \sum_{\beta \in \Gamma} A_{\alpha,\beta} m_\beta, \quad A_{\alpha,\beta} := A_{\alpha_1,\beta_1} \cdots A_{\alpha_d,\beta_d}.$$

FIGURE 2. Four-split of an irregular quad patch with $N = 6$ in a Doo-Sabin mesh.

Proof. For arbitrary \mathbf{P} , let $\mathbf{x} := B\mathbf{P}$ and $\mathbf{y}_k := \mathbf{x} \circ T_k = BA_k^t \mathbf{P}$ for $k \in K$. Using $\bar{\omega} = \bigcup \bar{\tau}_k$, the chain rule and the substitution rule, we find

$$\begin{aligned} M \cdot \mathbf{P} &= \sum_{k \in K} \int_{\tau_k} \det[\mathbf{x}, D\mathbf{x}] d\lambda = \sum_{k \in K} \int_{\omega} \det[\mathbf{y}, D\mathbf{y}_k DT_k^{-1}] \det DT_k d\lambda \\ &= \sum_{k \in K} \int_{\omega} \det[\mathbf{y}, D\mathbf{y}_k] d\lambda = \sum_{k \in K} M \cdot (A_k^t \mathbf{P}) = \sum_{k \in K} M[A_k] \cdot \mathbf{P}. \end{aligned}$$

Since this equality is valid for any \mathbf{P} , (3) follows. Equation (4) is easily verified by inspection. \square

It should be noted that the statement of the theorem does not rely on the fairly complicated definition of the coefficients m_α in terms of integrals over products of functions b_j and their derivatives. Rather, it reflects the refinement property of the function space in use.

Example 2 (resumption of Example 1). Let us go back to the example introduced above. Here, in the 2d case, M can be regarded as a skew-symmetric (3×3) -matrix, and the theorem yields the condition

$$M = A_1 M A_1^t + A_2 M A_2^t.$$

When solving this homogeneous system for M in the space of skew-symmetric matrices, as described later, we find a one-dimensional space of solutions,

$$(5) \quad M = h_1 M_1, \quad M_1 := \begin{bmatrix} 0 & 3 & 3 \\ -3 & 0 & 1 \\ -3 & -1 & 0 \end{bmatrix}, \quad h_1 \in \mathbb{R}.$$

\square

The constant in the example can be fixed if $V(\mathbf{x}) = M \cdot \mathbf{P}$ is known for a single, non-trivial case. We prepare the more detailed discussion of Section 3.1.3 by considering the following situation: If the trace $\mathbf{x}(\omega)$ is planar, i.e., contained in a hyperplane in \mathbb{R}^d , then the set

$$C(\mathbf{x}) := \{s\mathbf{x}(u) : s \in (0, 1), u \in \omega\}$$

is a cone with base $\mathbf{x}(\omega)$ and apex at the origin. Its volume is given by

$$\begin{aligned} \text{vol}(C(\mathbf{x})) &= \int_{C(\mathbf{x})} 1 dV = \int_0^1 \int_{\omega} \det[\mathbf{x}(u), s D\mathbf{x}(u)] duds \\ &= \int_0^1 \int_{\omega} s^{d-1} \det[\mathbf{x}(u), D\mathbf{x}(u)] duds = \frac{1}{d} \int_{\omega} \det[\mathbf{x}(u), D\mathbf{x}(u)] du = V(\mathbf{x}). \end{aligned}$$

That is, $V(\mathbf{x})$ is just the volume of the cone $C(\mathbf{x})$ and thus can be determined easily by geometric reasoning in many cases.

Example 3 (resumption of Example 2). Let $P_1^t = [2, 0, 0]$, $P_2^t = [0, 1, 0]$. Then the trace of the curve $\mathbf{x}(t) = B(t)\mathbf{P} = [2, t]$, $t \in (0, 1)$, is a straight line connecting the points $[2, 0]$ and $[2, 1]$. The corresponding cone $C(\mathbf{x})$ is a triangle with volume $V(\mathbf{x}) = 1$. Comparison with $V(\mathbf{x}) = P_1^t M P_2^t = 6h_1$ shows that $h_1 = 1/6$, and M is fixed. \square

2.4. Partial Refinability. The methodology introduced above covers a broad range of cases, but to facilitate, for instance, an efficient treatment of volumes bounded by subdivision surfaces of arbitrary topology, we need to generalize our setup. To explain the problem, we consider an irregular patch of a Doo-Sabin surface parametrized by $\mathbf{x} : (0, 1)^2 \rightarrow \mathbb{R}^3$, see Figure 2. It is determined by $n = N + 5$ control points, where N is the valency of the extraordinary vertex at issue. The function system B consists of N special functions and five biquadratic tensor product B-splines (TPBS). The standard four-split yields one irregular patch and three regular patches. While the new irregular patch can be expressed by the given functions B , a representation of the new regular ones require the complete set of nine biquadratic TPBS. It is possible to circumvent the problem by augmenting the given system B artificially by the four missing TPBS. However, this unnecessarily increases the size of the problem. A preferable solution is based on the observation that the trilinear forms corresponding to the three regular patches can be derived explicitly from the regular setup, which has to be treated anyway. Thus, these terms do not need to be determined again, but can be regarded as known. The following definition accounts for that situation:

Definition 3. *The functions $B = [b_1, \dots, b_n]$ are called partially refinable over ω if there exists a finite family of triples $(T_k, A_k, B_k), k \in K$, consisting of diffeomorphisms $T_k : \omega_k \rightarrow \tau_k \subset \omega_k$ defined on Jordan measurable domains $\omega_k \subset \mathbb{R}^{d-1}$ with $\det DT_k > 0$, constant $(n \times n_k)$ -matrices A_k , and vectors $B_k = [b_{k,1}, \dots, b_{k,n_k}]$ of real-valued functions defined on ω_k with the following properties:*

- Up to closure, the images τ_k form a partition of ω ,

$$\bar{\omega} = \bigcup_{k \in K} \bar{\tau}_k, \quad \tau_k \cap \tau_\ell = \emptyset, \quad k \neq \ell \in K.$$

- B restricted to τ_k can be reparametrized over ω by means of the functions B_k ,

$$B \circ T_k = B_k A_k^t, \quad k \in K.$$

The index set K is partitioned into the set

$$K' := \{k \in K : B_k = B, \omega_k = \omega\}$$

of indices referring to copies of the given functions, and the set $K'' := K \setminus K'$ of indices corresponding to auxiliary functions.

Clearly, refinability is a special case of partial refinability, characterized by $K'' = \emptyset$. On the other hand, $K' = \emptyset$ is also possible as demonstrated later in Example 15. Below, we assume that the d -linear forms M_k'' related to the auxiliary functions B_k by

$$M_k'' \cdot \mathbf{P} = V(B_k \mathbf{P}), \quad k \in K'', \quad \mathbf{P} \in \mathbb{R}^{n_k \times d},$$

are known, while the d -linear form M corresponding to the functions B is sought. The following formula interrelates these objects and can be regarded as an inhomogeneous system for determining M :

Theorem 4. *Let B be partially refinable according to the preceding definition. Then*

$$(6) \quad M = \sum_{k \in K'} M[A_k] + \sum_{k \in K''} M_k''[A_k].$$

Proof. The proof is a verbatim transcription of that of Theorem 2. □

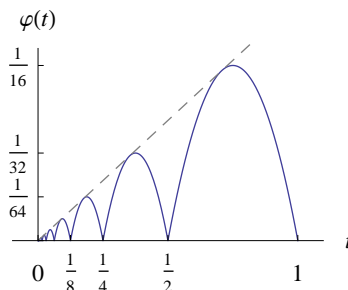
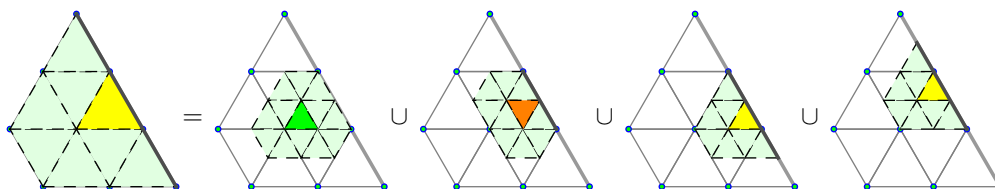
Typically, the inhomogeneous system (6) has a unique solution so that there is no need for calibration. The next example illustrates the method:

Example 4. With $a_\ell := 2^{-\ell}$, we define the function $\varphi : (0, 1) \rightarrow \mathbb{R}$ by

$$\varphi(t) := (t - a_{\ell+1})(a_\ell - t), \quad t \in [a_{\ell+1}, a_\ell], \quad \ell \in \mathbb{N}_0,$$

see Figure 3. The functions $B(t) := [\varphi(t), t]$ are not refinable over $\omega = (0, 1)$, but partially refinable with

$$T_1(t) = t/2, \quad T_2(t) = (t+1)/2, \quad A_1 = \frac{1}{4} \begin{bmatrix} 1 & 0 \\ 0 & 2 \end{bmatrix}, \quad A_2 = \frac{1}{4} \begin{bmatrix} 0 & 1 & -1 \\ 2 & 2 & 0 \end{bmatrix},$$

FIGURE 3. Function $\varphi : (0, 1) \rightarrow \mathbb{R}$ as used in Example 4.FIGURE 4. Refinement of a triangular patch adjacent to a sharp crease. The parametrizations $\mathbf{x}, \mathbf{y}_1, \dots, \mathbf{y}_4$ depend on the vertices \mathbf{P} , and $A_k^t \mathbf{P}$ as indicated.

and functions $B_1 := B, B_2(t) := [1, t, t^2]$. Thus, $K' = \{1\}, K'' = \{2\}$. The vector B_2 of auxiliary functions was already considered in Example 1. So we know

$$M_2'' = \frac{1}{6} \begin{bmatrix} 0 & 3 & 3 \\ -3 & 0 & 1 \\ -3 & -1 & 0 \end{bmatrix}, \quad M_2''[A_2] = A_2 M_2'' A_2^t = \frac{1}{48} \begin{bmatrix} 0 & 1 \\ -1 & 0 \end{bmatrix}.$$

The solution of the linear system $M = A_1 M A_1^t + M_2''[A_2]$ is unique and fixes M without calibration,

$$M = \frac{1}{42} \begin{bmatrix} 0 & 1 \\ -1 & 0 \end{bmatrix}.$$

It should be noted that in this case it would have been also possible (though quite laborious) to compute the specific value of the coefficient $m_{1,2} = -m_{2,1}$ directly by integration according to (2). \square

Example 5. Figure 4 shows a four-split of a triangle adjacent to a mesh boundary in the context of subdivision. The refinement results in three distinct types of patches. In order to apply the previous theorem, we encode the refinement with $K'' = \{1, 2\}$, and $K' = \{3, 4\}$. Based on the number of depicted control points, the matrix A_1 has dimensions 9×12 , A_2 is 9×10 , A_3 and A_4 are 9×9 . M may be determined by the linear system (6) if M_1 and M_2 are known. \square

2.5. Symmetry. In many cases, the arrangement of coefficients \mathbf{P} can be changed in certain ways without altering the modulus of the corresponding volume $V(B\mathbf{P})$. For instance, for a curve in Bernstein-Bézier form, reversing the order of control points results merely in a change of sign. Consequently, the coefficients of the bilinear form satisfy $m_\alpha = -m_{n+1-\alpha}$. The exploitation of symmetry properties of this type can be used to reduce the number of unknowns significantly when determining M . We formalize the concept as follows:

Definition 5. An $n \times n$ permutation matrix $\sigma \in \Pi_n$ is called a symmetry of the functions B if

$$(7) \quad V(B\mathbf{P}) = \det(\sigma) V(B\sigma\mathbf{P}), \quad \mathbf{P} \in \mathbb{R}^{n \times d}.$$

The set of all symmetries is denoted by Σ and called the symmetry group of B .

It is easy to verify that Σ is indeed a group with matrix multiplication as the group operation. In particular, $\sigma^{-1} = \sigma^t$. We identify the matrix σ with the one-line notation $\sigma(1), \dots, \sigma(n)$ of

the corresponding permutation of the set $\{1, \dots, n\}$. That is, the index $\sigma(i)$ is characterized by

$$\sigma_{i,j} = \delta_{\sigma(i),j}, \quad i, j = 1, \dots, n.$$

Further, we define $\sigma(\alpha) := [\sigma(\alpha_1), \dots, \sigma(\alpha_d)]$. Comparing the expressions

$$V(B\mathbf{P}) = \sum_{\alpha \in \Gamma} m_\alpha \mathbf{P}^\alpha = \sum_{\alpha \in \Gamma} m_{\sigma(\alpha)} \mathbf{P}^{\sigma(\alpha)}, \quad V(B\sigma\mathbf{P}) = \sum_{\alpha \in \Gamma} m_\alpha \mathbf{P}^{\sigma(\alpha)},$$

we find

$$m_\alpha = \det(\sigma) m_{\sigma(\alpha)}, \quad \alpha \in \Gamma, \quad \sigma \in \Sigma,$$

for the coefficients of M in case of symmetry. The linear space of all these Σ -symmetric d -linear forms which are also alternating is denoted by $\hat{\mathcal{S}}$. Comparison with (7) yields $M \cdot \mathbf{P} = \det(\sigma) M \cdot (\sigma\mathbf{P})$ for all elements $M \in \hat{\mathcal{S}}$, and $\sigma \in \Sigma$. By the group property of Σ , the same condition holds true for the inverse permutation σ^\dagger . Hence, we obtain the representation

$$\hat{\mathcal{S}} = \{M \in \mathcal{S} : M = \det(\sigma) M[\sigma], \sigma \in \Sigma\}.$$

Recalling notation introduced in Section 2.2, we derive a parametrization of this space using a bit of elementary group theory: Given any multi-index $\alpha \in \Gamma$ with pairwise different entries, there exists a unique permutation matrix $\omega_\alpha \in \Pi_d$ such that $\alpha\omega_\alpha \in \Lambda$ is ordered. Now, we define the map $G : \Sigma \times \Lambda \rightarrow \Lambda$ by

$$G(\sigma, \lambda) := \sigma(\lambda)\omega_{\sigma(\lambda)}, \quad \sigma \in \Sigma, \quad \lambda \in \Lambda.$$

Since $G(\text{Id}, \lambda) = \lambda$ and $G(\sigma_1, G(\sigma_2, \lambda)) = G(\sigma_1\sigma_2, \lambda)$ for all $\lambda \in \Lambda$ and $\sigma_1, \sigma_2 \in \Sigma$, this map defines a group action of Σ on Λ . The G -orbit of $\lambda \in \Lambda$ is defined as the set

$$\Omega(\lambda) := \{G(\sigma, \lambda) : \sigma \in \Sigma\},$$

and it is easy to see that there exist multi-indices $\lambda_1, \dots, \lambda_I$ such that

$$\Lambda = \bigcup_{i=1}^I \Omega(\lambda_i), \quad \Omega(\lambda_i) \cap \Omega(\lambda_j) = \emptyset, \quad i \neq j = 1, \dots, I.$$

That is, the G -orbits $\Omega(\lambda_i)$ form a partition of Λ . For each orbit, we define a d -linear form \hat{S}_i by

$$\hat{S}_i := \sum_{\sigma \in \Sigma} \det(\sigma) \det(\omega_\sigma) S_{G(\sigma, \lambda_i)}, \quad i = 1, \dots, I,$$

and it follows $\hat{\mathcal{S}} = \text{span}\{\hat{S}_i : i = 1, \dots, I\}$, and $\dim \hat{\mathcal{S}} \leq I$. The sought d -linear form M can now be written as

$$M = \hat{c}_1 \hat{S}_1 + \dots + \hat{c}_I \hat{S}_I.$$

Example 6. Let $B(t) := [(1-t)^2, 2t(1-t), t^2]$ be the quadratic Bernstein polynomials over $\omega = (0, 1)$, and let $T_1(t) := t/2$, $T_2(t) := (1+t)/2$. Reverting the order of control points \mathbf{P} causes nothing but a change of orientation of the corresponding curve. Hence, the symmetry group Σ contains the identity and the permutation

$$\sigma := \begin{bmatrix} 0 & 0 & 1 \\ 0 & 1 & 0 \\ 1 & 0 & 0 \end{bmatrix}, \quad \det(\sigma) = -1.$$

The G -orbits to the multi-indices $\lambda_1 = [1, 2]$ and $\lambda_2 = [1, 3]$ form a partition of Λ , and the corresponding bilinear forms generating $\hat{\mathcal{S}}$ are

$$\hat{S}_1 = \begin{bmatrix} 0 & 1 & 0 \\ -1 & 0 & 1 \\ 0 & -1 & 0 \end{bmatrix}, \quad \hat{S}_2 = \begin{bmatrix} 0 & 0 & 2 \\ 0 & 0 & 0 \\ -2 & 0 & 0 \end{bmatrix}.$$

Substitution of $M = \hat{c}_1 \hat{S}_1 + \hat{c}_2 \hat{S}_2$ in the equation $M = A_1 M A_1^\dagger + A_2 M A_2^\dagger$ yields a homogeneous system for the two unknowns $\hat{c}_1, \hat{c}_2 \in \mathbb{R}$. The solution is spanned by $\hat{c}_1 = 4, \hat{c}_2 = 1$ so that $M_1 = 4\hat{S}_1 + \hat{S}_2$. Calibration yields $M = M_1/12$. \square

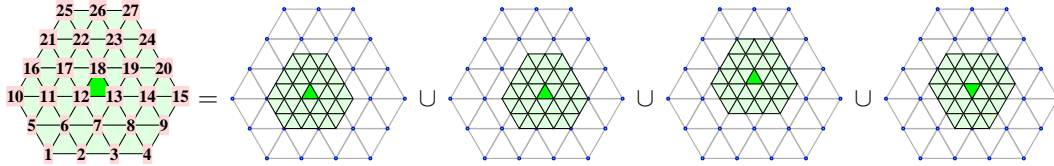


FIGURE 5. Four-split of a triangular patch in a Butterfly mesh. The vertices in the two-ring determine the surface parametrized by the center triangle.

Example 7. A regular patch in a *Butterfly*-mesh is defined by $|\mathbf{P}| = 27$ control points, see Figure 5. That means, $|\Lambda| = \binom{27}{3} = 2925$. The volume contribution by the surface patch is invariant under permutation of the control points by the dihedral group $\Sigma = D_3$ up to sign in the sense of (7). Using the computer, we find that there are $I = 509$ G -orbits, and further, that $\dim \hat{\mathcal{S}} = 508$. This discrepancy⁶ does not cause any problems in the subsequent treatment of the scheme. The size of the linear system to be solved is reduced by the factor $2925/509 \approx 5.7$, which is roughly the number of elements of the symmetry group D_3 . \square

3. ALGORITHMS

In this section, we elaborate on algorithms for determining M . First, we explain the basic algorithm for a refinable system B in some detail. Then, we discuss modifications to the basic algorithm in order to address partial refinability and symmetry.

3.1. Base Case. The algorithm for computing M in case of a refinable system of functions proceeds as follows:

1. Choose mappings $\{T_k : k \in K\}$ and corresponding matrices $\{A_k, k \in K\}$ providing a refinement of B over ω .
2. Set up the homogeneous system

$$(8) \quad M - \sum_{k \in K} M[A_k] = 0, \quad M \in \mathcal{S},$$

and compute a basis $\{M_1, \dots, M_r\}$ of the space \mathcal{M} of solutions.

3. Use at least r additional pieces of information to determine the coefficients h_1, \dots, h_r in the ansatz

$$M = h_1 M_1 + \dots + h_r M_r.$$

Before we discuss the three steps in turn, let us briefly comment on the role of the functions b_1, \dots, b_n . Apparently, these functions are never used explicitly in the algorithm so that it can be run without any knowledge about them. However, it is important to note that *existence* and sufficient smoothness of these functions must be assured to obtain meaningful results. Consider, for instance, a divergent uniform subdivision scheme. Then the algorithm will derive some bilinear form M from the refinement matrices A_1, A_2 , but there exist no corresponding curves and hence no planar sets whose areas could be addressed.

3.1.1. Refinement. In most applications, the functions B admit uniform binary refinement in a natural way. In particular, in the curve case $d = 2$, we may often choose $T_1(t) = t/2, T_2(t) = (t + 1)/2$ for $\omega = (0, 1)$. When generated by a standard subdivision scheme, as discussed in Section 4.1, the matrices A_1, A_2 are just the transposes of the two refinement matrices appearing in the matrix approach to smoothness analysis. In the surface case $d = 3$, the domain ω is typically (but not necessarily) a triangle or a quadrangle. Triangle-based subdivision algorithms like Loop or Butterfly admit refinement with respect to the standard four-split of the domain triangle, while two rounds of $\sqrt{3}$ -subdivision lead to a nine-split. Quad-based subdivision algorithms like Doo-Sabin or Catmull-Clark fit in with a four-split of the domain square. In all these cases, the coefficients of the matrices A_k can be read off easily from the subdivision rules in use.

⁶The discrepancy stems from the representative multi-index $(5, 12, 19)$ that is invariant under a mirror operation.

3.1.2. *The Homogeneous System.* To determine a basis of \mathcal{M} in practise, we vectorize the tensor equation $M = \sum_k M[A_k]$. This is done in the standard way by lexicographic ordering of the set Γ . More precisely, the vector $M^* \in \mathbb{R}^{n^d}$ corresponding to the tensor $M \in \mathbb{R}^{n \times \dots \times n}$ is defined by

$$M_{\alpha^*}^* := M_\alpha, \quad \alpha^* := 1 + \sum_{j=1}^d (\alpha_j - 1)n^{j-1} \in \mathbb{N}.$$

We call α^* the *linear index* corresponding to the multi-index $\alpha \in \Gamma$. The following lemma is a generalization of the well-known formula $(XYZ^t)^* = (X \otimes Z)Y^*$ for the vectorization of matrix products by means of the Kronecker product.

Lemma 6. *The vectorization of the d -linear form $M[A]$ in \mathbb{R}^n is given by*

$$(M[A])^* = A^{\otimes d} M^*,$$

where the $(n^d \times n^d)$ -matrix

$$A^{\otimes d} := A \otimes \dots \otimes A$$

is defined as the d -fold Kronecker product of A with itself.

Proof. The coefficients of the Kronecker power are given by $A_{\alpha^*, \beta^*}^{\otimes d} = A_{\alpha, \beta}$. Hence, by (4),

$$(A^{\otimes d} M^*)_{\alpha^*} = \sum_{\beta^*=1}^{n^d} A_{\alpha^*, \beta^*}^{\otimes d} M_{\beta^*}^* = \sum_{\beta \in \Gamma} A_{\alpha \beta} m_\alpha = (M[A])_{\alpha},$$

as requested. \square

Using this result, the vectorized form of (3) reads

$$A^* M^* = 0, \quad A^* := \text{Id} - \sum_{k \in K} A_k^{\otimes d}.$$

Still, the search for solutions has to be confined to the space \mathcal{S} of alternating forms, as introduced in Section 2.2. The linear index $\lambda^\times \in \{1, \dots, \binom{n}{d}\}$ corresponding to the multi-index $\lambda \in \Lambda$ is again obtained by lexicographic ordering of that set. Skipping the proof, we note that

$$\lambda^\times = \binom{n}{d} - \sum_{i=1}^d \binom{n - \lambda_i}{d + 1 - i}.$$

Since $\text{span}\{S_\lambda : \lambda \in \Lambda\} = \mathcal{S}$, it is $M = \sum_{\lambda \in \Lambda} c_\lambda S_\lambda$ for coefficients c_λ yet to be determined. We vectorize the d -linear forms S_λ and collect the resulting columns in the $(n^d \times \binom{n}{d})$ -matrix S^* such that the column with index λ^\times is just S_λ^* . Now, the space of alternating forms satisfying (8) is given by the solution of the linear system $A^* S^* C^* = 0$, where $C^* \in \mathbb{R}^{|\Lambda|}$ is the vectorization of the coefficients $c_\lambda, \lambda \in \Lambda$. The following theorem shows that this linear system can be replaced by an equivalent one which is significantly smaller. It has only $\binom{n}{d}$ instead of n^d rows and thus is square.

Theorem 7. *Let B be refinable according to Definition 1. Then the d -linear forms M satisfying (8) are characterized by $M^* = S^* C^*$ and $L^* C^* = 0$, where the system matrix is*

$$(9) \quad L^* := (S^*)^t A^* S^* \in \mathbb{R}^{\binom{n}{d} \times \binom{n}{d}}, \quad A^* := \text{Id} - \sum_{k \in K} A_k^{\otimes d}.$$

The coefficients of L^* are given by

$$L_{\lambda^\times, \mu^\times}^* = d! \delta_{\lambda, \mu} - \sum_{k \in K} \sum_{\pi_1 \in \Pi_d} \sum_{\pi_2 \in \Pi_d} \det(\pi_1) \det(\pi_2) (A_k)_{\lambda_{\pi_1}, \mu_{\pi_2}}, \quad \lambda, \mu \in \Lambda.$$

Proof. To verify the representation of M in terms of the kernel of L^* , we have to show for all $C^* \in \mathbb{R}^{|\Lambda|}$ with $L^* C^* = 0$ that also $A^* S^* C^* = 0$ holds. The d -linear form M with $M^* = S^* C^*$ is alternating, i.e., $M \in \mathcal{S}$. Then it is clear from the definition that $M[A_k]$ is alternating, too. Hence, $M - \sum_k M[A_k] \in \mathcal{S}$, implying that there exists some vector D^* satisfying

$$A^* S^* C^* = \left(M - \sum_{k \in K} M[A_k] \right)^* = S^* D^*.$$

Using $(S^*)^t S^* = d! \text{Id}$, the equation

$$0 = L^* C^* = (S^*)^t A^* S^* C^* = (S^*)^t S^* D^* = d! D^*$$

implies $D^* = 0$ and further $A^* S^* C^* = 0$. The formula for the coefficients is easily obtained by expanding the matrix product. \square

Example 8 (resumption of Example 3). The space \mathcal{S} of alternating bilinear forms in \mathbb{R}^3 is spanned by

$$S_{1,2} = \begin{bmatrix} 0 & 1 & 0 \\ -1 & 0 & 0 \\ 0 & 0 & 0 \end{bmatrix}, \quad S_{1,3} = \begin{bmatrix} 0 & 0 & 1 \\ 0 & 0 & 0 \\ -1 & 0 & 0 \end{bmatrix}, \quad S_{2,3} = \begin{bmatrix} 0 & 0 & 0 \\ 0 & 0 & 1 \\ 0 & -1 & 0 \end{bmatrix}.$$

The matrix $A^* = \text{Id} - A_1 \otimes A_1 - A_2 \otimes A_2$ has size 9×9 , while L^* is only 3×3 ,

$$L^* = \frac{4}{27} \begin{bmatrix} 0 & 0 & 0 \\ -6 & 6 & 0 \\ -1 & -2 & 9 \end{bmatrix}.$$

The kernel of this matrix has dimension 1 and is spanned by the vector $C^* = [3, 3, 1]^t$ so that we recover the solution

$$M = h_1 M_1, \quad M_1 := 3S_{1,2} + 3S_{1,3} + S_{2,3} = \begin{bmatrix} 0 & 3 & 3 \\ -3 & 0 & 1 \\ -3 & -1 & 0 \end{bmatrix},$$

presented already in (5). \square

3.1.3. Calibration. The dimension r of the space \mathcal{M} of d -linear forms satisfying (8) is at least 1 because it contains the d -linear form M defined in (1). Dimensions $r > 1$ are unlikely, though not excluded. In Example 4, we will deliberately construct such a case, but, as a matter of fact, we never encountered this situation in a realistic scenario. In particular, all cases discussed in the next section lead to a one-dimensional space. Calibration, as we call the process of determining the constants h_1, \dots, h_r in the ansatz $M = \sum_i h_i M_i$, can be accomplished by exploiting additional information about M .

The following strategy to gather such data proved to be sufficient in all cases we considered: It is based on seeking special configurations of coefficients \mathbf{P} such that the resulting values $M \cdot \mathbf{P}$ can be determined explicitly by geometric reasoning. Comparison with the ansatz then yields the unknowns. If, as it applies in many cases, the space of functions spanned by the functions B contains all constant and linear functions, the following strategy proves to be useful: A *standard configuration* of coefficients $\mathbf{P} = \mathbf{P}_1$ is characterized by $\mathbf{x}_1(u) := B(u)\mathbf{P}_1 = [d, u + c]$ for all $u \in \omega$ and some constant $c \in \mathbb{R}$. Hence, $\mathbf{x}_1(\omega) = \{d\} \times (\omega + c)$, and the cone $C(\mathbf{x}_1)$ has volume

$$V(\mathbf{x}_1) = M \cdot \mathbf{P}_1 = \text{vol}_{d-1}(\omega).$$

If $\mathcal{M} = \text{span}\{M_1\}$ is one-dimensional, this condition yields already the desired result,

$$(10) \quad M = h_1 M_1, \quad h_1 := \frac{\text{vol}_{d-1}(\omega)}{M_1 \cdot \mathbf{P}_1}.$$

Otherwise, if the dimension of \mathcal{M} is greater than 1, one has to resort to additional specific cases. As an alternative, one may search a different pattern of refinement and give it a try.

Example 9. We consider bilinear functions over the unit square,

$$B(u_1, u_2) = [(1 - u_1)(1 - u_2), (1 - u_1)u_2, u_1(1 - u_2), u_1u_2], \quad u \in (0, 1)^2.$$

When using as few as two mappings, e.g.,

$$T_1(u_1, u_2) = (u_1/2, u_2), \quad T_2(u_1, u_2) = ((u_1 + 1)/2, u_2),$$

then \mathcal{M} has dimension 2 because there is simply not enough information provided to resolve the structure of B completely. To remedy the situation, we add a less obvious special case to the standard configuration \mathbf{P}_1 ,

$$\mathbf{P}_1 := \begin{bmatrix} 3 & 3 & 3 & 3 \\ 0 & 0 & 1 & 1 \\ 0 & 1 & 0 & 1 \end{bmatrix}^t, \quad \mathbf{P}_2 := \begin{bmatrix} 3 & 3 & 3 & 3 \\ 0 & 0 & 2 & 1 \\ 0 & 1 & 0 & 1/2 \end{bmatrix}^t.$$

While $\mathbf{x}_1 = B\mathbf{P}_1$ parametrizes a square with side length 1, the trace of $\mathbf{x}_2 := B\mathbf{P}_2$ is a degenerate quad, namely the triangle with vertices $(3, 0, 0), (3, 2, 0), (3, 0, 1)$. The volumes of the corresponding cones are $V(\mathbf{x}_1) = V(\mathbf{x}_2) = 1$, what is just enough information to fix M within the two-dimensional space \mathcal{M} . We find

$$m_{1,2,3} = m_{1,2,4} = -m_{1,3,4} = -m_{2,3,4} = 1/12.$$

All other non-vanishing coefficients are related by alternation, $m_{\alpha\pi} = \det(\pi)m_\alpha, \alpha \in \Gamma$. The fact that \mathcal{M} is two-dimensional indicates a deficiency of the chosen refinement rather than an intrinsic problem with the given functions. And indeed, when using the standard four-split

$$(11) \quad \begin{aligned} T_1(u_1, u_2) &= (u_1, u_2)/2 & T_3(u_1, u_2) &= (u_1, u_2 + 1)/2 \\ T_2(u_1, u_2) &= (u_1 + 1, u_2)/2 & T_4(u_1, u_2) &= (u_1 + 1, u_2 + 1)/2 \end{aligned}$$

the dimension of \mathcal{M} becomes 1, as expected. Now, of course, the standard configuration \mathbf{P}_1 alone is sufficient for calibration according to (10). \square

3.2. Variants. Now, we discuss variants on the base algorithm in the case of partial refinability and symmetry.

3.2.1. Partial Refinability. The necessary modifications for the case of partial refinability are marginal.

Theorem 8. *Let B be partially refinable according to the Definition 3. Then the d -linear forms satisfying (6) are characterized by $M^* = S^*C^*$ and $L^*C^* = Y^*$, where the system matrix is*

$$L^* := (S^*)^t A^* S^*, \quad A^* := \text{Id} - \sum_{k \in K'} A_k^{\otimes d},$$

as before, and the right hand side is

$$Y^* := (S^*)^t \sum_{k \in K''} A_k^{\otimes d} (M_k'')^*.$$

Proof. Using Lemma 6, vectorization of (6) yields the system

$$A^* S^* C^* = Z^* := \sum_{k \in K''} A_k^{\otimes d} (M_k'')^*.$$

Multiplication with $(S^*)^t$ from the left proves necessity of the condition given in the theorem. To show that it is sufficient, assume that $L^*C^* = Y^*$. As in the proof of Theorem 7, there exists D^* such that $A^*S^*C^* = S^*D^*$. Regarding the right hand side Y^* , we note that the d -linear forms M_k'' , and hence also the $M_k''[A_k]$ are alternating. Hence, there exists a vector E^* such that $Z^* = S^*E^*$. Together, we have $(S^*)^t S^* D^* = (S^*)^t S^* E^*$. Because $(S^*)^t S^* = d! \text{Id}$, it follows $D^* = E^*$, and finally $A^*S^*C^* = S^*D^* = S^*E^* = Z^*$. \square

Example 10 (resumption of Example 4). With

$$A^* = \frac{1}{16} \begin{bmatrix} 15 & 0 & 0 & 0 \\ 0 & 14 & 0 & 0 \\ 0 & 0 & 14 & 0 \\ 0 & 0 & 0 & 12 \end{bmatrix}, \quad A_2 \otimes A_2 = \frac{1}{16} \begin{bmatrix} 0 & 0 & 0 & 0 & 1 & -1 & 0 & -1 & 1 \\ 0 & 0 & 0 & 2 & 2 & 0 & -2 & -2 & 0 \\ 0 & 2 & -2 & 0 & 2 & -2 & 0 & 0 & 0 \\ 4 & 4 & 0 & 4 & 4 & 0 & 0 & 0 & 0 \end{bmatrix},$$

and

$$S^* = [0, -1, 1, 0]^t, \quad (M_2'')^* = \frac{1}{6} [0, -3, -3, 3, 0, -1, 3, 1, 0]^t,$$

we obtain a linear system of size 1×1 with $L^* = 7/4$ and $Y^* = 1/24$. Its solution $C^* = 1/42$ yields the bilinear form $M = S/42$, as presented before. \square

3.2.2. *Symmetry.* In case of a non-trivial symmetry group Σ , there is a family \hat{S}_i , $i = 1, \dots, I$, spanning the space $\hat{\mathcal{S}}$ of Σ -symmetric d -linear forms. Collecting the vectorized versions in the $(n^d \times I)$ -matrix $\hat{S}^* := [\hat{S}_1^*, \dots, \hat{S}_I^*]$, the sought M can be written as $M^* = \hat{S}^* \hat{C}^*$ for some vector $\hat{C}^* \in \mathbb{R}^I$. Analogous to Theorem 7, we observe that the solutions of $A^* M^* = A^* \hat{S}^* \hat{C}^* = 0$ satisfy

$$\hat{L}^* \hat{C}^* = 0, \quad \hat{L}^* := (\hat{S}^*)^t A^* \hat{S}^* \in \mathbb{R}^{I \times I}.$$

The coefficients of \hat{L}^* are given by

$$(12) \quad \hat{L}_{i,j}^* = d_i \delta_{i,j} - \sum_{k \in K} \sum_{\sigma_1, \sigma_2 \in \Sigma} \sum_{\pi_1, \pi_2 \in \Pi_d} \det(\sigma_1 \sigma_2) \det(\omega_{\sigma_1} \omega_{\sigma_2} \pi_1 \pi_2) (A_k)_{G(\sigma_1 \lambda_i) \pi_1, G(\sigma_2 \lambda_j) \pi_2},$$

where $i, j \in I$, and $d_i := \|\hat{S}_i^*\|^2$ is the squared Euclidean norm of \hat{S}_i^* .

Example 11 (resumption of Example 6). The bilinear forms \hat{S}_1, \hat{S}_2 generating $\hat{\mathcal{S}}$ yield

$$\hat{S}^* = \begin{bmatrix} 0 & -1 & 0 & 1 & 0 & -1 & 0 & 1 & 0 \\ 0 & 0 & -2 & 0 & 0 & 0 & 2 & 0 & 0 \end{bmatrix}^t.$$

The kernel of the resulting matrix $\hat{L}^* = \begin{bmatrix} 1 & -4 \\ -1 & 4 \end{bmatrix}$ is spanned by the vector $[4, 1]^t$ so that $M_1 = 4\hat{S}_1 + \hat{S}_2$. Calibration yields $M = M_1/12$. \square

It should be noted that exploiting symmetry can reduce the costs of solving a given problem considerably, and can well make the difference between the capacities of a standard PC and a mainframe. As a rule of thumb, the number sizes of the matrices L^* and \hat{L}^* are related by $\binom{n}{d}/I \approx \#\Sigma$, where $\#\Sigma$ is the number of elements of the symmetry group. Consequently, the required storage and computation time are reduced by the factors $(\#\Sigma)^2$ and $(\#\Sigma)^3$, respectively. For larger problems, these savings are significant, even if there exists only one non-trivial symmetry so that $\#\Sigma = 2$.

4. CASE STUDIES

In this section, we discuss a series of examples that are relevant for applications and/or illustrate the potential of our approach. The amount of data which the first author has collected during extensive studies of these and further examples is far too copious to be presented here in detail. Instead, this material as well as some Mathematica source code is available for download⁷.

4.1. **Binary Subdivision Curves.** In this section, we discuss uniform and non-uniform binary subdivision curves. Subdivision schemes of arbitrary arity can also be treated by our approach, but are not considered here.

4.1.1. *Uniform Univariate Schemes.* Let the boundary curve $\partial\Omega$ of the set $\Omega \subset \mathbb{R}^2$ be generated by a binary, stationary, and uniform C^1 subdivision scheme with finite masks from a periodic sequence $\mathbf{p}^1, \dots, \mathbf{p}^N \in \mathbb{R}^2$ of control points. Then we partition $\partial\Omega$ into N segments $\partial\Omega_j$. Suppressing the subscript j , the natural parametrization of any segment is given by some function $\mathbf{x} : (0, 1) \rightarrow \mathbb{R}^2$ which is the linear combination of functions⁸ $B = [b_1, \dots, b_n]$ with a subsequence \mathbf{P} of n consecutive control points, $\mathbf{x} = B\mathbf{P}$. The number n of functions is related to the size of the masks. When applying the subdivision scheme to the points \mathbf{P} , we obtain a vector $\mathbf{Q} = [\mathbf{q}_1; \dots; \mathbf{q}_{n+1}]$ of $n+1$ new control points. The vectors formed by the first n and the last n points of \mathbf{Q} are denoted by $\mathbf{Q}_1 := [\mathbf{q}_1; \dots; \mathbf{q}_n]$ and $\mathbf{Q}_2 := [\mathbf{q}_2; \dots; \mathbf{q}_{n+1}]$, respectively. They are related to \mathbf{Q} by a pair of square matrices with columns containing the subdivision masks padded with zeros,

$$\mathbf{Q}_1 := A_1^t \mathbf{P}, \quad \mathbf{Q}_2 := A_2^t \mathbf{P}.$$

Using the two-split $T_1(t) = t/2$, $T_2(t) = (1+t)/2$ of the interval $\omega = (0, 1)$, we obtain the reparametrization $\mathbf{x} \circ T_k = B A_k^t \mathbf{P}$ and the refinement equations

$$B \circ T_k = B A_k^t, \quad k \in \{1, 2\}.$$

⁷<http://www.hakenberg.de/subdivision/subdivision.htm>

⁸If $\varphi : \mathbb{R} \rightarrow \mathbb{R}$ is the basic limit function of the subdivision scheme with $\text{supp } \varphi = [0, n]$, then b_k is the restriction of $\varphi(\cdot + n - k)$ to the unit interval, but this fact is not needed here.

Hence, the matrix $A^* = \text{Id} - A_1 \otimes A_1 - A_2 \otimes A_2$ can be generated easily. As for calibration, we recall that the subdivision scheme is assumed to be C^1 . Thus, it is known to generate constant and linear functions from constant and linear sequences of control points, respectively. In particular,

$$B(t)\mathbf{P}_1 = [2, t + c], \quad \mathbf{P}_1 := \begin{bmatrix} 2 & 2 & \cdots & 2 \\ 1 & 2 & \cdots & n \end{bmatrix}^t,$$

for some constant $c \in \mathbb{R}$ so that \mathbf{P}_1 defines a standard configuration, independent of the specific scheme.

Example 12. For B-splines of degree $k \in \mathbb{N}$ with integer knots and the standard two-split of $\omega = (0, 1)$ the refinement matrices are well known,

$$(A_1)_{i,j} = \frac{1}{2^k} \binom{k+1}{2i-j}, \quad (A_2)_{i,j} = \frac{1}{2^k} \binom{k+1}{2i-j-1}, \quad i, j = 1, \dots, k+1.$$

For the corresponding bilinear forms $M_{\mathbb{B}}^k$ we obtain for instance

$$M_{\mathbb{B}}^1 = \frac{1}{2} \begin{bmatrix} 0 & -1 \\ 1 & 0 \end{bmatrix}, \quad M_{\mathbb{B}}^2 = \frac{1}{24} \begin{bmatrix} 0 & -5 & -1 \\ 5 & 0 & -5 \\ 1 & 5 & 0 \end{bmatrix}, \quad M_{\mathbb{B}}^3 = \frac{1}{720} \begin{bmatrix} 0 & -31 & -28 & -1 \\ 31 & 0 & -183 & -28 \\ 28 & 183 & 0 & -31 \\ 1 & 28 & 31 & 0 \end{bmatrix}.$$

In all these cases, the kernel of L^* is one-dimensional so that calibration according to (10) determines $M_{\mathbb{B}}^k$ uniquely. Since the B-splines considered here are polynomials on $\omega = (0, 1)$, the coefficients of $M_{\mathbb{B}}^k$ can alternatively be calculated using integration according to (2). \square

Example 13. The interpolatory four-point scheme (FPS) with tension parameter $w \in (0, 0.19273\dots)$ generates C^1 -limit curves, see [9]. The mask $[-w, 1/2 + w, 1/2 + w, -w]$ determines new edge points. The support of the scheme is $n = 6$. The basis functions in $b_j \in B$ for $j = 1, \dots, n$ do not have a closed-form expression, which rules out integration (2). The refinement matrices are

$$(13) \quad A_1 = \begin{bmatrix} 0 & -w & 0 & 0 & 0 & 0 \\ 1 & w' & 0 & -w & 0 & 0 \\ 0 & w' & 1 & w' & 0 & -w \\ 0 & -w & 0 & w' & 1 & w' \\ 0 & 0 & 0 & -w & 0 & w' \\ 0 & 0 & 0 & 0 & 0 & -w \end{bmatrix}, \quad A_2 = \begin{bmatrix} -w & 0 & 0 & 0 & 0 & 0 \\ w' & 0 & -w & 0 & 0 & 0 \\ w' & 1 & w' & 0 & -w & 0 \\ -w & 0 & w' & 1 & w' & 0 \\ 0 & 0 & -w & 0 & w' & 1 \\ 0 & 0 & 0 & 0 & -w & 0 \end{bmatrix}$$

where $w' := 1/2 + w$. Using a computer algebra system, we find $(M_{\text{FPS}})_{i,j} = \frac{1}{F} m_{i,j}$ with common denominator $F = -96w^5 + 144w^4 - 102w^3 + 72w^2 - 24w + 6$, and coefficients $m_{1,2} = 8w^6 + 8w^5 + 4w^4 + 4w^3$, $m_{1,3} = -16w^5 + 6w^4 - 10w^3 + 2w^2$, $m_{1,4} = -6w^4 + 2w^3 - 2w^2$, $m_{1,5} = 4w^3 - 4w^4$, $m_{1,6} = 8w^5 - 8w^6$, $m_{2,3} = -12w^5 + 16w^4 - 12w^3 + 6w^2 - 4w$, $m_{2,4} = 8w^5 - 6w^4 + 14w^3 - 2w^2 + 4w$, $m_{2,5} = 8w^6 + 12w^5 - 2w^4 - 2w^3 - 4w^2$, and $m_{3,4} = 12w^5 - 38w^4 + 13w^3 - 24w^2 + 4w - 3$. Further, $m_{i,j} = m_{7-j,7-i} = -m_{j,i}$ for all $i, j \in \{1, \dots, 6\}$.

The curve generated from the four corner points of the unit square encloses an area of $\frac{16\omega^3 + 11\omega^2 + 7\omega + 3}{48\omega^4 - 24\omega^3 + 27\omega^2 - 9\omega + 3}$. The area form for tension parameter $w = 1/16$ is already derived in [19], page 166. \square

4.1.2. Non-Uniform Univariate Schemes. Now, we consider two non-uniform schemes. These schemes have little relevance in applications, but, from a structural point of view, they can be regarded as one-dimensional analogies to subdivision schemes for surfaces of arbitrary topology. Thus, the subsequent arguments may serve as a preparation for the bivariate cases discussed later on.

Example 14. We consider a simple modification to cubic B-Spline subdivision. By replacing the averaging mask $[1, 6, 1]/8$ with $[0, 1, 0]$ at selected *crease* vertices, these control points are interpolated by the limit curve. The three control points \mathbf{P} that determine a segment adjacent to the crease vertex, see Figure 6, are subdivided by

$$A_1 = \frac{1}{8} \begin{bmatrix} 4 & 1 & 0 & 0 \\ 4 & 6 & 4 & 0 \\ 0 & 1 & 4 & 8 \end{bmatrix}, \quad A_2 = \frac{1}{8} \begin{bmatrix} 1 & 0 & 0 \\ 6 & 4 & 0 \\ 1 & 4 & 8 \end{bmatrix}.$$

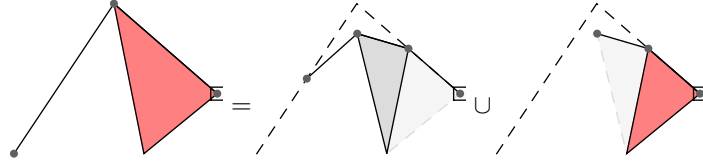


FIGURE 6. Decomposition of a segment adjacent to a crease vertex (*red*) into a regular cubic B-spline segment (*gray*) and a new segment adjacent to a crease vertex (*red*). The limit curve is not shown.

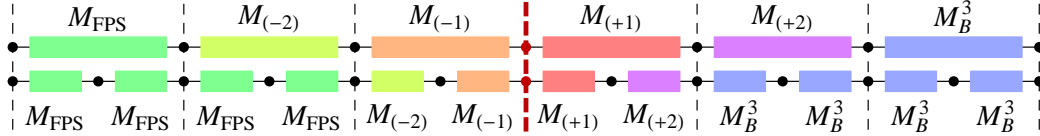


FIGURE 7. The four bilinear forms $M_{(-2)}$, $M_{(-1)}$, $M_{(+1)}$, and $M_{(+2)}$ determine the area contribution of the four non-uniform curve segments close to the interface. The recursive relation follows from overlapping the segments before and after one round of subdivision.

It is easy to see that the left segment of the limit curve is just a cubic polynomial written in B-spline form, which has been considered before. The right segment, however, consists of an infinite sequence of cubic pieces. This is exactly the situation of partial refinability as discussed in sections 2.4 and 3.2.1. The equation that relates the area forms before and after one round of subdivision is $M = M_B^3[A_1] + M[A_2]$ where M_B^3 is familiar from Example 12, and M is the sought 3×3 alternating bilinear form. Writing out the equations gives

$$\begin{bmatrix} -15 & 0 & 0 \\ 1 & -14 & 0 \\ 5 & 12 & -8 \end{bmatrix} \begin{bmatrix} m_{1,2} \\ m_{1,3} \\ m_{2,3} \end{bmatrix} = \frac{1}{24} \begin{bmatrix} 15 \\ 13 \\ 55 \end{bmatrix} \Rightarrow M = \frac{1}{24} \begin{bmatrix} 0 & -1 & -1 \\ 1 & 0 & -9 \\ 1 & 9 & 0 \end{bmatrix}.$$

□

Example 15. In [13], page 21, Levin derives a C^1 curve subdivision scheme that blends between the FPS with tension parameter $w = 1/16$ and cubic B-spline subdivision. Figure 7 visualizes the refinement of three segments to either side of the interface. For $k \in \{1, 2\}$, the subdivision matrices $A_k^{(-3)}$ are stated in (13), the matrices $A_k^{(-2)}$, $A_k^{(-1)}$ have dimension 6×6 , the matrices $A_k^{(+1)}$ are 5×5 , and $A_k^{(+2)}$ are 5×4 . The segment (-2) is refined into two FPS patches. The segment $(+2)$ is refined into two cubic B-spline segments. That means the alternating bilinear forms $M_{(-2)}$, $M_{(+2)}$ follow explicitly from forms for the respective uniform schemes and are computed first:

$$\begin{aligned} M_{(-2)} &= M_{\text{FPS}}[A_1^{(-2)}] + M_{\text{FPS}}[A_2^{(-2)}] \\ M_{(+2)} &= M_B^3[A_1^{(+2)}] + M_B^3[A_2^{(+2)}] \end{aligned}$$

Subsequently, the forms for the segments adjacent to the interface vertex (-1) , and $(+1)$ follow from solving linear systems that use the previously obtained $M_{(-2)}$, $M_{(+2)}$:

$$\begin{aligned} M_{(-1)} &= M_{(-2)}[A_1^{(-1)}] + M_{(-1)}[A_2^{(-1)}] \\ M_{(+1)} &= M_{(+1)}[A_1^{(+1)}] + M_{(+2)}[A_2^{(+1)}] \end{aligned}$$

The resulting forms contain lengthy fractions and are omitted here. □

4.2. Binary Subdivision Surfaces. In this section, we discuss a series of variants on binary subdivision algorithms for surfaces, both quad and triangle based, both uniform and non-uniform.

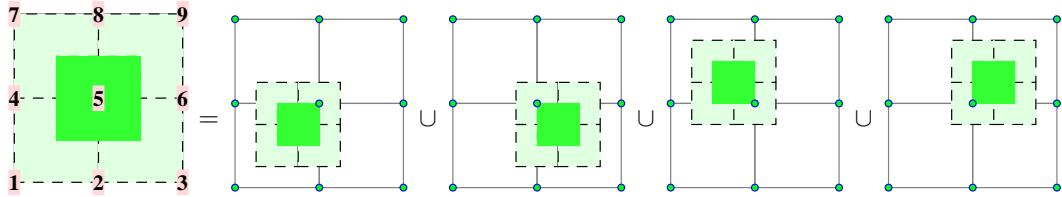


FIGURE 8. A biquadratic TPBS patch depends on $3 \cdot 3 = 9$ control points \mathbf{P} . Refinement is based on a $2 \times 2 = 4$ -split.

4.2.1. *Tensor Product Surfaces.* Bivariate bases on rectangular domains are often defined as tensor product of univariate functions. If B^1, B^2 are two (possibly coinciding) function systems with n_1 and n_2 elements, respectively, then the corresponding tensor product system B is defined by

$$B(u_1, u_2) = B^1(u_1) \otimes B^2(u_2) = [b_1^1(u_1)b_1^2(u_2), b_1^1(u_1)b_2^2(u_2), \dots, b_{n_1}^1(u_1)b_{n_2}^2(u_2)].$$

The following theorem states that refinability of the univariate bases implies refinability of their tensor product, and shows how to establish the according rules in a convenient way:

Theorem 9. *For $i \in \{1, 2\}$, let B^i be a univariate function system which is refinable over the interval ω^i with pairs $(T_{k_i}^i, A_{k_i}^i), k_i \in K_i$. Then the tensor product system $B := B^1 \otimes B^2$ is refinable over $\omega := \omega^1 \times \omega^2$ with*

$$T_k(u_1, u_2) := (T_{k_1}^1(u_1), T_{k_2}^2(u_2)), \quad A_k := A_{k_1}^1 \otimes A_{k_2}^2, \quad k = (k_1, k_2) \in K := K_1 \times K_2.$$

Proof. The partitioning of ω into sets $T_k(\omega_{k_1}^1 \times \omega_{k_2}^2), k \in K$, is obvious. Further, the mixed-product property yields

$$\begin{aligned} B \circ T_k &= (B^1 \circ T_{k_1}^1) \otimes (B^2 \circ T_{k_2}^2) = (B^1 \cdot (A_{k_1}^1)^t) \otimes (B^2 \cdot (A_{k_2}^2)^t) \\ &= (B^1 \otimes B^2)((A_{k_1}^1)^t \otimes (A_{k_2}^2)^t) = (B^1 \otimes B^2)(A_{k_1}^1 \otimes A_{k_2}^2)^t = BA_k^t \end{aligned}$$

for any $k \in K$, as claimed. \square

Clearly, a similar result applies to higher-dimensional tensor products as well, and also variants concerning partial refinability can be derived easily. For later reference, we consider some low degree TPBS surfaces. In principle, there are three different approaches to determine the corresponding volume forms

- (1) Integration of the coefficients of M using (1), what is feasible since all basis functions are polynomials.
- (2) Computation of the nullspace of L^* as defined in (9) and subsequent calibration according to (10).
- (3) Computation of the nullspace of \hat{L}^* as defined in (12) using the dihedral symmetry group $\Sigma = D_4$ and subsequent calibration according to (10).

But of course, we will focus on options 2 and 3. We will always specify only one sample entry for comparison; complete results can be found online.

Example 16 (resumption of Example 12). Bilinear TPBS on the unit square are related to the functions B^1 introduced in the preceding example by

$$B(u_1, u_2) = B^1(u_1) \otimes B^1(u_2) = [(1 - u_1)(1 - u_2), (1 - u_1)u_2, u_1(1 - u_2), u_1u_2],$$

what is just the system discussed in Example 2. The four diffeomorphisms T_1, \dots, T_4 given there are related to $T_1^1(t) = T_1^2(t) = t/2, T_2^1(t) = T_2^2(t) = (1+t)/2$ by the formula given in the theorem and relabelling. Also the four matrices can be found easily using $A_k^1 = A_k^2$, for instance

$$A_{2,1} = A_2^1 \otimes A_1^1 = \begin{bmatrix} 1/2 & 0 \\ 1/2 & 1 \end{bmatrix} \otimes \begin{bmatrix} 1 & 1/2 \\ 0 & 1/2 \end{bmatrix} = \frac{1}{4} \begin{bmatrix} 2 & 1 & 0 & 0 \\ 0 & 1 & 0 & 0 \\ 2 & 1 & 4 & 2 \\ 0 & 1 & 0 & 2 \end{bmatrix}.$$

\square

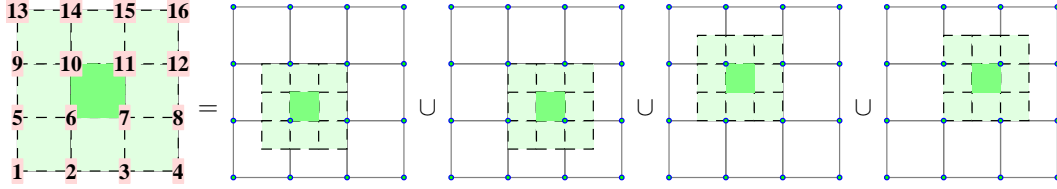


FIGURE 9. Refinement of a bicubic TPBS where 16 control points \mathbf{P} determine the surface parametrized by the unit square.

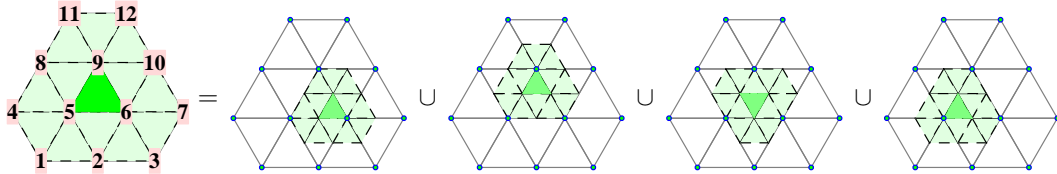


FIGURE 10. Four-split of a triangular patch in a quartic three-direction box spline. The vertices in the 1-ring determine the surface parametrized by the center triangle ω .

Example 17. We consider biquadratic TPBS on the unit square, as illustrated in Figure 8. The total number of coefficients to be determined is $9^3 = 729$. The size of L^* is $\binom{9}{3} = 84$, while the size of \hat{L}^* is only 14. Aside from the zeros which are enforced by the alternating property, there exists further non-trivial zeros. They are generated by the coefficient $m_{1,2,3} = 0$. The remaining coefficients are signed copies of only 13 distinct numbers. A sample value is $m_{2,4,5} = -121/4800$. The form M is already listed in [18], pages 82–86. \square

Example 18. Now, we consider bicubic TPBS on the unit square. The total number of coefficients to be determined is $16^3 = 4096$. The size of L^* is $\binom{16}{3} = 560$, while the size of \hat{L}^* is only 75. With indexing as in Figure 9, the non-trivial zeros are generated by the coefficients $m_{1,2,3} = m_{1,2,4} = m_{2,6,10} = m_{2,6,14} = 0$. The remaining coefficients are signed copies of only 71 distinct numbers, where the largest one is $m_{6,7,10} = \frac{22344529}{1219276800}$. \square

The practical limitations of the approach presented here become apparent if we consider the complexity of the problem to be solved in the case of tensor product surfaces of significantly higher bidegree $g \gg 1$. Here, the number of basis functions is $n = (g + 1)^2$. Hence, the dimension of the matrix L^* is $\ell := \binom{n}{3} \approx g^6/6$, and the number of coefficients to be stored is $\ell^2 \approx g^{12}/36$. Solving the linear system via factorization needs $\ell^3/3 \approx g^{18}/648$ operations. The dihedral symmetry group D_4 has 8 elements. Thus, the matrix \hat{L}^* has only size $\hat{\ell} \approx \ell/8$ so that storage requirements are approximatively reduced by the factor $8^2 = 64$, and computation time by the factor $8^3 = 512$. This is a significant saving, but even then, already modest values of g yield a problem beyond the reach of current computer technology.

4.2.2. Triangle-Based Uniform Subdivision. Now, we consider triangular surface patches which are generated by uniform binary subdivision.

Example 19. Three-direction box splines, sometimes also called triangular B-splines, are another natural extension of univariate B-splines to the bivariate case. They consist of triangular polynomial pieces and thus can be treated by elementary integration according to (1), but also by using the refinement rules, which are typically very simple for low degrees. In Figure 10, we see the pattern for a C^2 quartic box spline. This case is of particular interest since it is used for the regular parts of the mesh in Loop subdivision. Here, the size of L^* is $\binom{12}{3} = 220$. Exploiting the dihedral symmetry group $\Sigma = D_3$ yields the matrix \hat{L}^* , which has only size 43. After calibration with (10), we find for instance $m_{5,6,9} = 34091/1425600$. \square

Example 20 (resumption of Example 7). We continue our discussion of the Butterfly scheme. Here, the volume form cannot be determined via straightforward integration because the basis

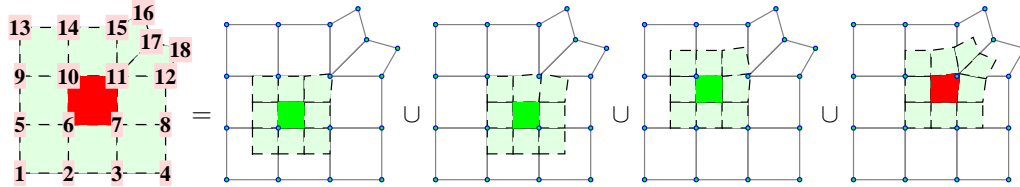


FIGURE 11. Decomposition of a non-regular quad patch in a Catmull-Clark mesh.

functions do not have a closed-form expression. The size of L^* is $\binom{27}{3} = 2925$, while \hat{L}^* has only size $\dim \hat{\mathcal{S}} = 508$. Similar to the FPS, the subdivision weights may be subject to a tension parameter $w \in \mathbb{R}$, but we fix the natural choice $w = 1/16$. In this case, the limit surface is C^1 . The non-trivial zeros are generated by $m_{1,j,27} = 0$ for $j \in \{2, 3, \dots, 13\} \cup \{16, 17\}$ and $m_{1,15,25} = 0$. The coefficient with the largest amplitude is $m_{12,13,18} \approx 0.151032$, while the smallest one is $m_{9,1,25} \approx 1.45624E - 16$. The latter value is not a zero perturbed by roundoff errors, but the floating point evaluation of a fraction with 74 digits in the numerator and 90 digits in the denominator. \square

4.2.3. Non-Uniform Subdivision Schemes. Non-uniform refinement rules for subdivision *curves*, as discussed in Examples 14 and 15, do not appear frequently in practice. In *surface* modeling however, meshes are likely to feature irregularities and the designers of surface subdivision schemes are creative to cope with them in order to produce smooth limit surfaces. To name just a few schemes currently in use, there are those based on quads [1, 3, 11] and triangles [15, 4, 12], but also mixed schemes [14, 17] and schemes with crease rules [10, 2]. Refinability or partial refinability is a common feature of all these schemes so that the corresponding volume forms can be determined by our approach. What follows is a tour de force through the different types. For more details, we refer to the online material mentioned above.

Example 21 (resumption of Example 17). The Doo-Sabin algorithm is a generalization of bi-quadratic TPBS subdivision. An extraordinary patch including a vertex of valency $N \geq 3, N \neq 4$, is defined by $n = N + 5$ control points. Five of them correspond to standard TPBS, while the other N are special as they consist of an infinite number of polynomial pieces, faintly resembling the univariate case discussed in Example 4. Assuming that the extraordinary vertex corresponds to the parameter $u_1 = u_2 = 1$, the map T_4 from the standard four-split (11) yields a new extraordinary patch, while the other three yield regular ones. That means, in (6) $K'' = \{1, 2, 3\}$, $K' = \{4\}$, and M'' corresponds to the uniform case $N = 4$ derived earlier. A refinement of a patch with $N = 6$ is shown in Figure 2. The symmetry group consists of the identity and a reflection across the diagonal containing the extraordinary point. \square

Example 22 (resumption of Example 18). The Catmull-Clark algorithm is a generalization of bicubic TPBS subdivision. An extraordinary patch including a vertex of valency $N \geq 3, N \neq 4$, is defined by $n = 2N + 8$ control points. Seven of them correspond to standard TPBS, while the other are special as they consist of an infinite number of polynomial pieces. Assuming that the extraordinary vertex corresponds to the parameter $u_1 = u_2 = 1$, the map T_4 from the standard four-split (11) yields a new extraordinary patch, while the other three yield regular ones. That means, in (6) $K'' = \{1, 2, 3\}$, $K' = \{4\}$, and M'' corresponds to the uniform patch $N = 4$ derived earlier. For valency $N = 5$, the refinement of a patch is depicted in Figure 11. Here, the largest coefficient is $m_{10,7,11} \approx 0.0202676$, and the smallest positive coefficient is $m_{16,1,18} \approx 1.31029E - 10$. Again, the symmetry group consists of the identity and a reflection across the diagonal containing the extraordinary point. \square

Example 23 (resumption of Example 19). The Loop algorithm is a generalization of quartic box-spline subdivision. An extraordinary patch including a vertex of valency $N \geq 3, N \neq 6$, is defined by $n = N + 6$ control points. Five of them coincide with the uniform scenario, while the other are special. We refine ω as illustrated by Figure 12: the map T_k for $k \in K' = \{4\}$ yields a new extraordinary patch, while the other three $K'' = \{1, 2, 3\}$ yield regular ones. In (6),

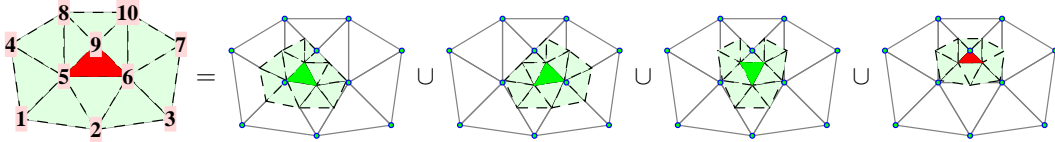


FIGURE 12. Four-split of a extraordinary triangular patch in a Loop mesh.

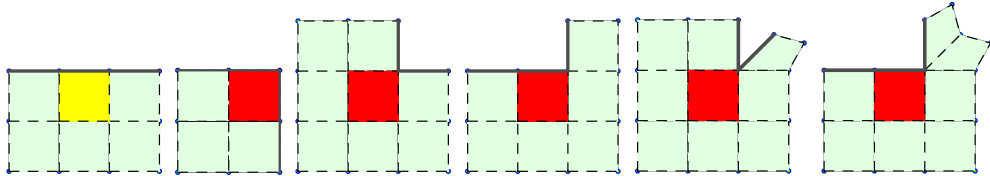


FIGURE 13. Classification and ordering of patch types adjacent to a sharp crease for the successive derivation of corresponding volume forms.

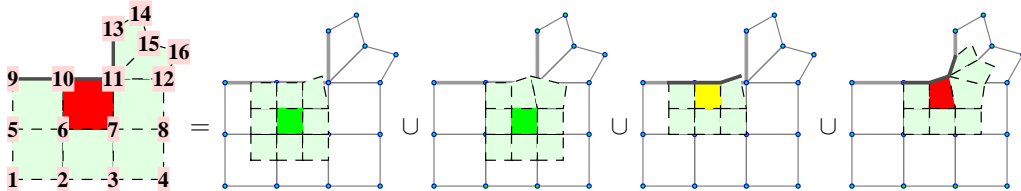


FIGURE 14. Decomposition of a quad patch adjacent to a crease.

M'' corresponds to $N = 6$ and was derived earlier. For valency $N = 4$, the largest coefficient is $m_{5,6,9} \approx 0.0216354$, and the smallest positive coefficients are $m_{1,2,7} = m_{2,3,4} = 1/3991680$. \square

In [7], we discuss the three mentioned algorithms in detail, carry out the computation of volume forms up to a certain valency, and state additional sample coefficient values.

4.2.4. *Schemes with Sharp Creases.* [10] extends the Loop-scheme to produce sharp creases along selected edge-cycles. Later, [2] introduces the same modification to Catmull-Clark subdivision. In [8], we discuss these algorithms in detail.

Example 24. We consider the algorithm suggested in [2]. The refinement rules along the crease edges are simply cubic B-spline subdivision for curves. Because control points from “beyond” the crease do not affect a patch, the support of the original schemes is reduced. As already encountered in Example 15, the derivation of a volume form for a patch adjacent to a crease may depend on another volume form for a patch adjacent to a crease. A line-up of patch types is required so that refinement only drafts patch types derived earlier. Figure 13 shows the line-up for the scheme suggested in [2]. We consider the refinement illustrated in Figure 14. Here, $K'' = \{1, 2, 3\}$, $K' = \{4\}$, A_1 , and A_2 have dimensions 16×16 , A_3 is 16×12 , and A_4 is 16×16 . The forms $M''_1 = M''_2$ are known from Example 18. Assuming M''_3 is provided from a prior derivation, the sought M follows from (6). The largest coefficient is $m_{6,11,10} \approx 0.035485$, the smallest positive entry is $m_{1,14,4} = \frac{256}{53133856452440253}$. \square

5. CONCLUSION

We suggest a method for determining the volume of a subset of \mathbb{R}^d in the case that its boundary is the union of a set of refinable patches. The contribution of each patch can be expressed in terms of a d -linear form which is narrowed by an underdetermined linear system derived from the refinement equations of the patch. The remaining degrees of freedom – this is typically only one – can be fixed by comparison with certain elementary configurations. Symmetries can be used to reduce the complexity of the linear system. In particular, our approach is applicable to planar sets bounded by subdivision curves and to spatial sets bounded by subdivision algorithms like

Catmull-Clark, Loop, or Butterfly, but also non-uniform variants like crease rules are covered. Applications of our theory include for instance the deformation of subdivision surfaces under preservation of volume.

In the more application-oriented reports [5] and [6], we have generalized the ideas presented here to the computation of higher order moments of sets bounded by subdivision curves and surfaces respectively. Higher order moments are required, for instance, to determine centroids or inertia tensors. While being similar from a structural point of view, the big challenge here is to cope with the rapidly growing complexity of the linear systems to be solved, coming along with an unfavorable loss of inherent symmetries.

Acknowledgement: We would like to thank Scott Schaefer for fruitful discussions and comments, and for providing sample 3d-meshes.

REFERENCES

- [1] E. Catmull and J. Clark. Recursively generated B-spline surfaces on arbitrary topological meshes. *Computer Aided Design*, 10:350–355, 1978.
- [2] T. DeRose, M. Kass, and T. Truong. Subdivision surfaces in character animation. In *Proceedings of the 25th Annual Conference on Computer Graphics and Interactive Techniques*, SIGGRAPH '98, pages 85–94, New York, NY, USA, 1998. ACM.
- [3] D. Doo and M.A. Sabin. Behaviour of recursive subdivision surfaces near extraordinary points. *Computer Aided Design*, 10:356–360, 1978.
- [4] N. Dyn, D. Levin, and J.A. Gregory. A butterfly subdivision scheme for surface interpolation with tension control. *ACM Transactions on Graphics*, 9:160–169, 1990.
- [5] J. Hakenberg, U. Reif, S. Schaefer, and J. Warren. Moments defined by subdivision curves. viXra:1407.0163, 2014.
- [6] J. Hakenberg, U. Reif, S. Schaefer, and J. Warren. On moments of sets bounded by subdivision surfaces. viXra:1408.0070, 2014.
- [7] J. Hakenberg, U. Reif, S. Schaefer, and J. Warren. Volume enclosed by subdivision surfaces. viXra:1405.0012, 2014.
- [8] J. Hakenberg, U. Reif, S. Schaefer, and J. Warren. Volume enclosed by subdivision surfaces with sharp creases. viXra:1406.0060, 2014.
- [9] J. Hechler, B. Mößner, and U. Reif. C^1 -continuity of the generalized four-point scheme. *Linear Algebra and its Applications*, 430(11–12):3019–3029, 2009.
- [10] H. Hoppe, T. DeRose, T. Duchamp, M. Halstead, H. Jin, J. McDonald, J. Schweitzer, and W. Stuetzle. Piecewise smooth surface reconstruction. In *Proceedings of the 21st Annual Conference on Computer Graphics and Interactive Techniques*, SIGGRAPH '94, pages 295–302, New York, NY, USA, 1994. ACM.
- [11] L. Kobbelt. Interpolatory subdivision on open quadrilateral nets with arbitrary topology. In *Computer Graphics Forum*, pages 409–420, 1996.
- [12] L. Kobbelt. $\sqrt{3}$ -subdivision. In *Proceedings of the 27th Annual Conference on Computer Graphics and Interactive Techniques*, SIGGRAPH '00, pages 103–112, New York, NY, USA, 2000. ACM Press/Addison-Wesley Publishing Co.
- [13] A. Levin. Polynomial generation and quasi-interpolation in stationary non-uniform subdivision. *Comput. Aided Geom. Des.*, 20(1):41–60, March 2003.
- [14] A. Levin and D. Levin. Analysis of quasi-uniform subdivision. *Applied and Computational Harmonic Analysis*, 15(1):18–32, 2003.
- [15] Ch.T. Loop. Smooth subdivision for surfaces based on triangles. Master's thesis, University of Utah, 1987.
- [16] J. Peters and A. Nasri. Computing volumes of solids enclosed by recursive subdivision surfaces. 16(3), September 1997.
- [17] S. Schaefer and J. Warren. On C^2 triangle/quad subdivision. *ACM Trans. Graph.*, 24(1):28–36, January 2005.
- [18] B. Schwald. Exakte Volumenberechnung von durch Doo-Sabin-Flächen begrenzten Körpern. Diplomarbeit, Universität Stuttgart, Math. Inst. A, 1999.
- [19] J. Warren and H. Weimer. *Subdivision Methods for Geometric Design: A Constructive Approach*. Morgan Kaufmann Publishers Inc., San Francisco, CA, USA, 1st edition, 2001.